

Transition Experiments on a Slender Cone at Mach 3

Jörgen Olsson

Experimental Aerodynamics

FFA, The Aeronautical Research Institute of Sweden

Bromma

Sweden

ABSTRACT

An experimental investigation of boundary layer stability and transition on a slender cone at Mach number 3 has been performed as a part of Sweden's participation in the German Hypersonic Technology Programme. The experiment involved wind tunnel quality assessments, boundary layer surveys, natural transition detection, influences of small angles of attack, and influence of nose bluntness on stability and transition.

Natural transition location, transition length and amplification rates have been found for three different nose tips and at small angles of attack.

INTRODUCTION

During the late 1980's and early 1990's there was an increased interest in hypersonic spaceplanes. With the one-stage-to-orbit NASP project as the main US activity and the two-stage-to-orbit SÄNGER project as one of the main European activities. Both projects have since been cancelled and replaced by more limited efforts. These projects started new research programmes in various topics in hypersonic aerodynamics.

Within the SÄNGER project a 10 year plan for hypersonic stability and transition research was drawn up with the aim to have reliable prediction methods available by the early 2000's. The plan involved both experimental and theoretical work and was shared between research organisations and universities in Germany and Sweden. In Sweden most of the theoretical work was conducted at KTH^{1,11}, the Royal Institute of Technology, Stockholm, and the experimental work was made by FFA. The experimental work started with a simple flat plate test in order to learn the technique with hot wires in supersonic flow³.

This paper presents the second experimental part of the work done in Sweden.

EXPERIMENTAL SET UP AND INSTRUMENTATION

The investigation was conducted on a 500 [mm] long slender cone with an half angle of seven degrees. The cone was made of steel and had a wall thickness of 5 [mm]. The frustum could be divided in a plane offset and parallel to the symmetry axis thus providing one side of the frustum with undisturbed flow while still allowing for further instrumentation. Of particular interest was nose bluntness effects, thus the cone could be configured with either a sharp nose or with one of two blunted noses with half sphere-conical geometry and radii's of 6 and 10 [mm] respectively. The geometry of the cone was chosen to conform with the experiments by Stetson et. al.^{7,8} using the same half cone angle and nose radius Reynolds number for the blunt cases but running at a lower Mach number.

Measurements on the cone was made by traversing a 1.2 [mm] long hot wire of 5 [mm] diameter through the boundary layer at several downstream positions. Additional flow data was obtained by traversing a flattened Pitot tube through the boundary layer and measurements of the static pressure field around the cone.

The measurements were made in FFA's S5 suck down wind tunnel which has a test section size of 460*580 [mm], and uses exchangeable fixed nozzles for each Mach number. Running at Mach = 3 and with atmospheric stagnation pressure and temperature, the Reynolds number, based on a unit length of one meter, is 7.7 millions. The run time was approximately one minute allowing for a full traverse through the boundary layer at one x-position. The free stream condition in the tunnel gave edge condition on the

cone according to inviscid theory⁴ with $M_e = 2.823$, $R_e = 8.61$ millions and velocity, $U_e = 598$ [m/s].

Natural transition of the boundary layer was investigated for the three noses on the windward and the leeward side at angles of attack of 0, 1 and 2 degrees.

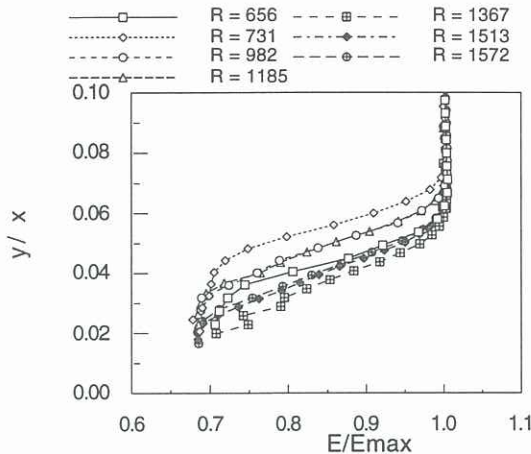


Figure 1. Normalized mean profiles for sharp cone at zero angle of attack.

HOT WIRE ANALYSIS

According to King's law, often referred to in hot wire anemometry, the electrical power needed to keep the wire at constant temperature, or current, is proportional to the local Reynolds number. This means for compressible flow that a hot wire measures mass flow variations. However, close to $M = 1$ the hot wire is highly Mach number dependent, a circumstance which makes calibration and subsequent analysis of fluctuating quantities difficult for hot wires in transonic flow. At higher Mach numbers, between 1.3 and 4.5, hot wires can measure mass flow fluctuations accurately. The independence from Mach number in this range is due to the hypersonic freeze phenomenon⁸. On a seven degree cone at $M_\infty = 3$ the boundary layer is mainly supersonic. The measurements in this experiment showed that amplification of disturbances occurred in the supersonic part of the boundary layer. This fact made it possible to use a simplified analysis of hot wire data.

Although it is possible to calibrate the wire by following the procedure of Smits et. al.⁵ it is still possible to get qualitative overall boundary layer and transition characteristics from the raw output voltage. These characteristics include boundary layer thickness, where the boundary layer becomes subsonic, overall disturbance levels leading to determination of onset and end of transition.

For determining the amplification rate calibration is not strictly necessary due to the fact that measurements were made at the same mean voltage for each x-position thus assuring that the hot wire have the same sensitivity. The non-dimensional amplification rate is defined as:

$$-\alpha_i = \frac{1}{2A} \frac{\partial A}{\partial R},$$

where $R (= \sqrt{R_x})$ is the Reynolds number based on Blasius length and A the maximum disturbance rms amplitude of mass flow, which can be substituted for maximum rms voltage amplitude as only small disturbances around the mean is considered. In order to be able to calculate the derivative a second-order polynomial was fitted to the data in the streamwise direction following the procedure of Wendt¹⁰.

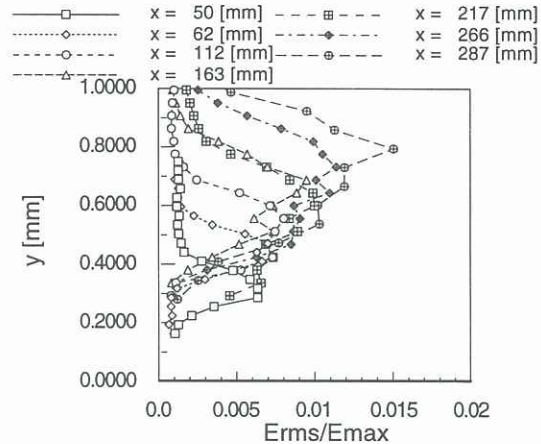


Figure 2. Normalised rms profiles for sharp cone at zero angle of attack.

RESULTS

Profiles was measured in the boundary layer from 50 [mm] up to the end of the cone. For each x-position 10240 samples were recorded at 20 y-positions in the boundary layer. Sampling rate was 100 kHz and a anti-aliasing filter with 48dB/octave damping above 50 kHz was used.

For the sharp cone at zero angle of attack the part where linear growth of disturbances was found, reached from 50 [mm] up to 287 [mm] corresponding to a Reynolds number of 600 to 1500. Fig. 1 shows the 7 mean profiles measured in this range. The raw voltage is normalised with the corresponding free stream value and the y-coordinat is normalised with the square root of x. In previous unpublished measurements these profiles have been found to be self similar. In this case the lack of self similarity is believed to be caused by incorrectly determined wall distance. It can be seen in the figure that the profiles have the same slope except for the x-position most upstream which is influenced by the proximity to the apex. For the other cases with sharp and blunt cones at angle of attack, profiles showed self similar behaviour with the wall distance normalised as above.

Fig. 2 shows the corresponding broad band rms of the voltage for the mean profiles of fig. 1. The raw voltage rms is normalised with the free stream mean voltage while the wall distance and x-position is shown in dimensional form to indicate the location of the

measurements and the thickness of the boundary layer. The growth of the disturbance level for increasing streamwise distance is clearly seen. The peak rms value is found at about 75% of the boundary layer thickness, in agreement with Wendt et.al.¹¹, and it moves away from the wall with increasing boundary layer thickness.

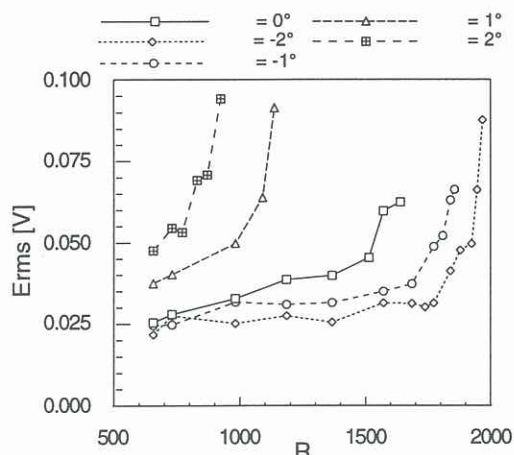


Figure 3. Overall rms of disturbance fluctuations for sharp cone at angle of attack.

From the measured mean and rms profiles transition location and transition length could be found. At an angle of attack of zero degrees for the sharp cone, natural transition was found to occur between $x = 320$ [mm] and $x = 420$ [mm] corresponding to a transition Reynolds number range of 2.5 to 3.2 millions. The peak in disturbance amplitude is found at $x = 400$ [mm]. For the blunt cases transition was moved downstream with onset starting 30 to 40 [mm] downstream of the sharp nose case.

At the small angles of attack investigated, transition moved upstream on the lee side and downstream on the wind side. For the wind side the behaviour was almost linear for the angles of attack investigated while on the lee side the behaviour is highly non-linear already for small angles.

Fig. 3 shows the development of the broad band of the maximum disturbance in the boundary layer for the region where disturbances grow linearly for the sharp cone at zero angle of attack. The stabilising of the windward boundary layer is seen as well as the rapid non-linear development on the leeward side.

Calculating the amplitude spectra for the hot wire signals at the peak of rms fluctuations for each profile shows the growth of different frequency components. Fig. 4 shows the rms amplitude spectra ($\Delta f = 97.66$ [Hz]) as function of Reynolds number. It is not evident from this figure where the maximum growth occurs due to the high dynamic range of the signal. Calculating growth rates (Fig. 5) clearly shows where the highest amplification of disturbances occur. The disturbance level of the spectra at low frequencies is high but have low growth rate which decreases downstream. The highest growth occurs in a broad band hump between

15 to 50 [kHz] with the crest around 32 [kHz]. The lack of data around 15 [kHz] is due to spurious electronic noise centred around this frequency which led to exclusion of the data.

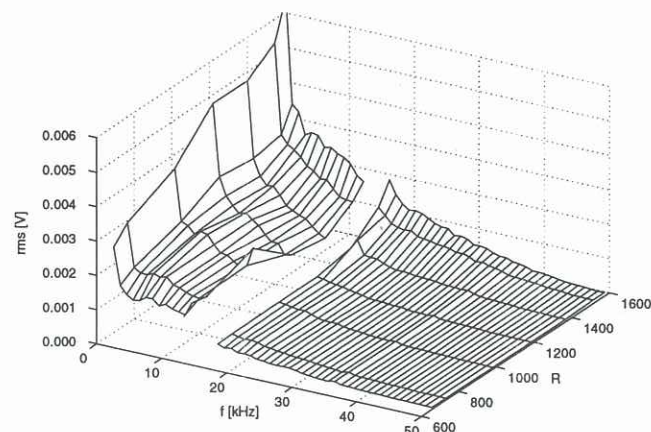


Figure 4. Amplitude spectra for sharp cone $\alpha = 0^\circ$

Comparing amplification rates at a Reynolds number of 1200 for the sharp cone and the two blunt cases shows that the broad band hump of high amplification rate is moved to lower frequencies (fig. 6). For the $r = 6$ [mm] case the extent is from 1 to 25 [kHz] with the crest at 12 [kHz]. At $r = 10$ [mm] the range is from 1 to 22 [kHz] with the crest around 10 [kHz] for both these cases there is a second peak, at 26-27 [kHz] for $r = 6$ [mm] and at 24-25 [kHz] for $r = 10$ [mm]. The significance of this peak is as yet not explained.

For the cone at angle of attack only the windward data could be analysed due to the rapid onset of non-linear growth on the lee side. Fig. 7 shows a comparison of the zero angle of attack case with the two angles of attack tested. The comparison is made for a fixed Reynolds number of 1200. The amplification rate is lower for the two angle of attack cases but the frequency extent of the high amplification rate hump is comparable to the zero angle of attack case.

CONCLUSIONS

The transition Reynolds number found on the sharp cone at zero angle of attack was low and comparable to Kings² data for noisy flow conditions. This implies that the free stream disturbance level in the wind tunnel is comparable to most conventional supersonic tunnels. For a quiet tunnel the transition Reynolds number is at least a factor two higher². An increase of transition Reynolds number with nose bluntness was observed but with a less dramatic increase than found in earlier work^{6,8}, 10-15% instead of 70%. The level of bluntness was not large enough to reverse this trend. Likewise was the trend of transition Reynolds number movement at angle of attack similar to both theoretical¹ and previous experimental findings^{5,6}.

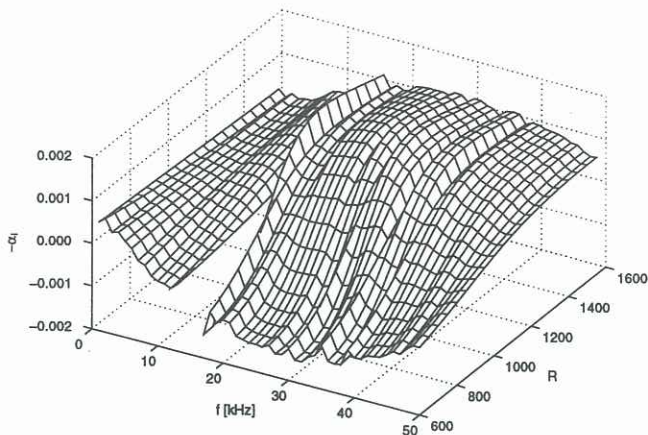


Figure 5. Amplification rate for sharp cone $\alpha = 0^\circ$

No theoretical analysis of the cases presented here has yet been done which prevents comparison with linear theory. Most theoretical and experimental work found in the literature deals with higher Mach numbers where the second mode is dominant. Calculating amplification rates for the sharp cone showed a broad frequency band for which amplification takes place. On the wind side of the sharp cone at angle of attack, maximum amplification rates moves to higher Reynolds numbers. For the two blunt cases the amplification rates found showed a growth at lower frequencies than for the sharp cone. This is in contrast to the results by Stetson et. al⁸.

A theoretical analysis is needed to further analyse the experimental data. This will hopefully be done in the near future.

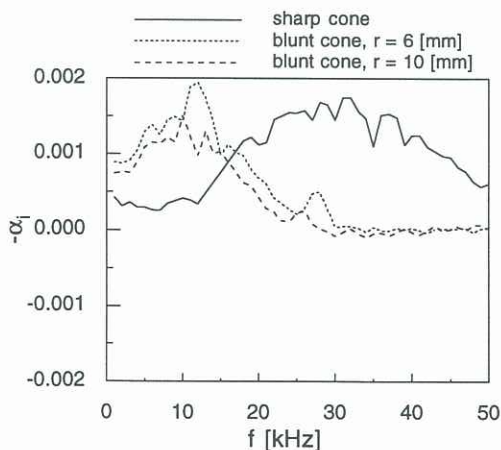


Figure 6. Amplification rate at $R = 1200$ and zero angle for three nose bluntnesses.

REFERENCES

1. Hanifi, A. & Dahlkild, A. A., "Some Stability Characteristics of the Boundary Layer on a Yawed Cone", AIAA-93-3048, July, 1993.

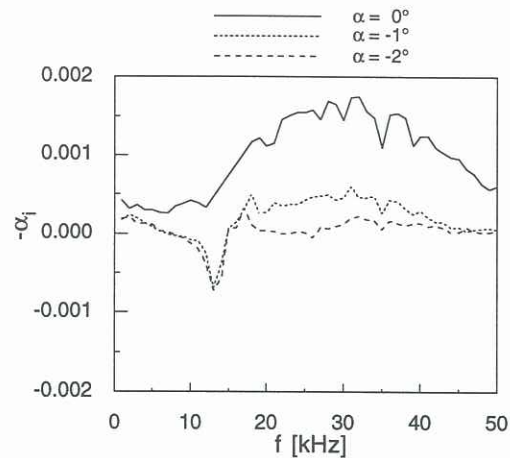


Figure 7. Amplification rate at $R = 1200$ for sharp cone at three angles of attack.

2. King, R. E., "Three-Dimensional Boundary Layer Transition on a Cone at Mach 3.5", Exp. in Fluids 13, 1992, 305-314.
3. Olsson J., "Boundary Layer Measurements on a Flat Plate at Mach 3", FFA TN-1993-34, 1993.
4. Simms J. L., "Tables for Supersonic Flow Around Right Circular Cones at Zero Angle of Attack", NASA SP-3004, 1964.
5. Smits, A. J., Hayakawa, K., & Muck, K. C., "Constant-Temperature Hot-Wire Anemometer Practice in Supersonic flows, Part 1: The Normal Wire", Exp. in Fluids 1, 1983, 83-92.
6. Softley, E. J., "Boundary Layer Transition on Hypersonic Blunt, Slender Cones", AIAA-69-705, June 1969.
7. Spina, E. F. & McGinley, C. B., "Constant-Temperature Anemometry in Hypersonic Flow: Critical Issues and Sample Results", Exp. In Fluids 17, (1994), 365-374.
8. Stetson, K. F., Thompson, E. R., Donaldson, J. C. & Siler, L. G., "Laminar Boundary Layer Stability Experiments on a Cone at Mach 8, Part 2: Blunt Cone", AIAA-84-0006, January 1984.
9. Stetson, K. F., Thompson, E. R., Donaldson, J. C. & Siler, L. G., "Laminar Boundary Layer Stability Experiments on a Cone at Mach 8, Part 3: Sharp Cone at Angle of Attack", AIAA-85-0492, January 1985.
10. Wendt, V., "Experimentell Untersuchung der Instabilität von ebenen und konischen laminaren Hyperschallgrenzschichten", DLR-FB 93-56, PhD. Thesis, 1993.
11. Wendt, V., Simen, M., & Hanifi, A., "An Experimental and Theoretical Investigation of Instabilities in Hypersonic Flat Plate Boundary Layer Flow", Phys. Fluids 7, April 1995.